

# Ablation of Nkx2-5 at mid-embryonic stage results in premature lethality and cardiac malformation

Ryota Terada<sup>1</sup>, Sonisha Warren<sup>1</sup>, Jonathan T. Lu<sup>2</sup>, Kenneth R. Chien<sup>3</sup>, Andy Wessels<sup>4</sup>, and Hideko Kasahara<sup>1\*</sup>

<sup>1</sup>Department of Physiology and Functional Genomics, University of Florida College of Medicine, 1600 SW Archer Rd. M540, Gainesville, FL 32610-0274, USA; <sup>2</sup>Cardiology Division, Department of Medicine, Columbia University, New York, NY, USA; <sup>3</sup>Cardiovascular Research Center, Massachusetts General Hospital, Boston, MA, USA; and <sup>4</sup>Department of Regenerative Medicine and Cell Biology, Medical University of South Carolina, Charleston, SC, USA

Received 15 September 2010; revised 22 January 2011; accepted 28 January 2011; online publish-ahead-of-print 1 February 2011

Time for primary review: 15 days

## Aims

Human congenital heart disease linked to mutations in the homeobox transcription factor, NKX2-5, is characterized by cardiac anomalies, including atrial and ventricular septal defects as well as conduction and occasional defects in contractility. In the mouse, homozygous germline deletion of Nkx2-5 gene results in death around E10.5. It is, however, not established whether Nkx2-5 is necessary for cardiac development beyond this embryonic stage. Because human NKX2-5 mutations are related to septum secundum type atrial septal defects (ASD), we hypothesized that Nkx2-5 deficiency during the processes of septum secundum formation may cause cardiac anomalies; thus, we analysed mice with tamoxifen-inducible Nkx2-5 ablation beginning at E12.5 when the septum secundum starts to develop.

## Methods and results

Using tamoxifen-inducible Nkx2-5 gene-targeted mice, this study demonstrates that Nkx2-5 ablation beginning at E12.5 results in embryonic death by E17.5. Analysis of mutant embryos at E16.5 shows arrhythmias, contraction defects, and cardiac malformations, including ASD. Quantitative measurements using serial section histology and three-dimensional reconstruction demonstrate growth retardation of the septum secundum and enlarged foramen ovale in Nkx2-5-ablated embryos. Functional cardiac defects may be attributed to abnormal expression of transcripts critical for conduction and contraction, including cardiac voltage-gated Na<sup>+</sup> channel pore-forming  $\alpha$ -subunit (Na<sub>v</sub>1.5- $\alpha$ ), gap junction protein connexin40, cardiac myosin light chain kinase, and sarcolipin within 4 days after tamoxifen injection.

## Conclusion

Nkx2-5 is necessary for survival after the mid-embryonic stage for cardiac function and formation by regulating the expression of its downstream target genes.

## Keywords

Genetics • Heart defects • Congenital • Conduction • Contractility

## 1. Introduction

Congenital heart defects are the most prevalent malformations in the foetal and neonatal period, affecting ~1% of live births.<sup>1,2</sup> While the aetiology of most defects remains unknown, a number of genetic and environmental factors have been determined to be involved in a subset of congenital abnormalities.<sup>3</sup> One gene identified to be associated with congenital heart disease is the homeobox transcription factor, NKX2-5. Heterozygous NKX2-5 mutations cause a spectrum of cardiac anomalies, including atrial septal defects (ASD), ventricular septal defects (VSD), and Tetralogy of Fallot, with ~80% penetrance in ASD and/or VSD as well as nearly complete penetrance of

postnatal progressive conduction defects and occasional left ventricular dysfunction.<sup>4–7</sup>

Nkx2-5 is highly conserved among species and is one of the earliest cardiogenic markers with expression continuing throughout adulthood.<sup>8–12</sup> Germline-targeted disruption of Nkx2-5 in mice causes embryonic lethality around embryonic (E) Day 10.5 with retarded cardiac development.<sup>13,14</sup> Previous studies using mice with homozygous deletion of floxed-Nkx2-5 alleles using Cre-recombinase under the control of myosin light chain 2v (ventricular isoform), in which Nkx2-5 is ablated in cells committed to ventricular cardiomyocytes after around E8.0, did not demonstrate cardiac structural anomalies.<sup>15</sup> These mice survive to adulthood and demonstrate

\* Corresponding author. Tel: +1 352 846 1503; fax: +1 352 846 0270, Email: hkasahar@phys.med.ufl.edu

conduction defects and cardiac hypertrophy. Multiple heterozygous Nkx2-5 knockout mouse lines have been analysed and demonstrate substantially different disease penetrance and severity with the reported incidence of ASD between ~1 and 18%.<sup>16–19</sup> This is likely due to different targeting strategies, mouse genetic backgrounds, and analytical methodologies. To explain mechanisms of the cardiac defects related to Nkx2-5, further investigation of animal models that demonstrate cardiac defects similar to those seen in human patients are valuable.

The atrial septum is a complex structure that, in the late foetal and postnatal hearts, consists of two components: a septum primum and a septum secundum.<sup>20</sup> Before birth, a functional opening in the atrial septum, the foramen ovale, is essential for a right-left shunt in the atria. After birth, however, as the lungs become operational and the pulmonary circulation is established, the foramen ovale normally closes as a result of changes in the relative pressure in two atrial chambers. Abnormal formation of components of the atrial septum can result in ASD. In the mouse, septum primum starts to develop at E10.0 and septum secundum starts to grow at E12.5.<sup>21</sup> Because human NKX2-5 mutations are related to septum secundum type ASD, we hypothesized that Nkx2-5 deficiency during the processes of septum secundum formation may cause cardiac anomalies. Mice with tamoxifen-inducible Nkx2-5 deficiency beginning at E12.5 indeed demonstrate abnormal morphology of septum secundum resulting in an enlarged foramen ovale, contraction and conduction abnormalities, and death by E17.5. These results indicate that Nkx2-5 is necessary for survival after mid-embryonic stage for cardiac function and formation of the four-chamber heart by regulating the expression of its downstream target genes.

## 2. Methods

For details on methods, see Supplementary material online.

### 2.1 Inducible Nkx2-5 knockout mice

Floxed-Nkx2-5 mice<sup>15</sup> were bred with transgenic mice carrying the Cre-ER<sup>TM</sup> gene under the control of cytomegalovirus (CMV) promoter.<sup>22</sup> Details of mouse generation and experimental were described previously.<sup>23</sup> To delete the floxed-Nkx2-5 gene, tamoxifen (0.1 mg/g body weight, ip) was injected once or 2 consecutive days into pregnant mice at noon at E12.5. Embryonic staging was determined by standard methods counting the morning on which the vaginal plug was found as E0.5. Embryos were analysed 4 days later around noon, and analyses were completed within 2 h. The investigation conforms to the Guide for the Care and Use of Laboratory Animals published by the US National Institutes of Health (NIH Publication No. 85–23, revised 1996). All animal care protocols fully conformed to the Association for the Assessment and Accreditation of Laboratory Animal Care, with approval from the University of Florida Institutional Animal Care and Use Committee.

### 2.2 Histological analysis and western blotting

X-gal staining of frozen sections was performed according to the standard protocol.<sup>24</sup> Immunostaining and western blotting were performed with the primary antibodies or cell death detection system listed in the Supplementary material online. Acetylcholine esterase (AChE) staining in frozen tissue sections was performed as described previously<sup>25</sup> with some modifications (see Supplementary material online). Fluorescent microscopic images were obtained using ZEISS Axiovert200M, and diaminobenzidine-stained tissue section images were obtained using Nikon Eclipse 50i attached to a charge-coupled device (CCD) camera. Digitalized images were utilized for measurement using Image J software.

### 2.3 Ultrasound imaging

B- and M-mode ultrasound imaging of foetal hearts was performed on pregnant mice anaesthetized with isoflurane (1–1.5%) using an ultrasound biomicroscope with a 35 MHz transducer (VisualSonics, Toronto, Canada). The pregnant mice were placed on a platform maintained at 37°C, with a heart rate between 348 and 448 b.p.m. Mice with litter sizes <6 were utilized for echocardiography, which was identified by initial ultrasound scanning. Foetal heart rate was obtained from M-mode imaging of ventricular contraction (number of heart beats/time). Ventricular wall thickness, distance of ventricular cavities, and area size were determined by two-dimensional imaging of both end-diastole and end-systole.

### 2.4 Cardiac three-dimensional reconstruction

We followed the methodology described previously<sup>26</sup> with minor modifications. Paraffin-embedded tissues sections (5 µm thickness) were stained with haematoxylin-eosin and digitalized with a CCD camera (QImaging, Micropublisher, BC Canada) attached to Nikon SMZ800 microscope. The images were processed from 24 to 8 bits followed by alignment, labelling, and surface smoothing using the Amira program (Visage Imaging, Inc. San Diego, CA, USA, version 5.3).

### 2.5 Real-time reverse transcriptase–polymerase chain reaction

Real-time reverse transcriptase–polymerase chain reaction (RT–PCR) was performed using inventoried Taqman Gene Expression Assays listed in the Supplementary material online (Applied Biosystems). Duplicate experiments were averaged.

### 2.6 Simultaneous recording of cardiac contraction and Ca<sup>2+</sup>

Cardiomyocytes isolated from E15.5 embryonic hearts were studied for simultaneous measurements of cardiomyocyte contraction and Ca<sup>2+</sup> measurement as described previously.<sup>27</sup>

### 2.7 Statistical analysis

Values among groups were compared using ANOVA and Fisher's protected least significant difference post hoc test (StatView version 5.01).  $P < 0.05$  was considered significant.

## 3. Results

### 3.1 Inducible Nkx2-5 ablation by tamoxifen injection beginning at E12.5 results in death by E17.5

With respect to the pathogenesis of human congenital cardiac disease associated with human NKX2-5 mutations, the role of Nkx2-5 during embryonic stages in cardiac morphogenesis remains to be elucidated. To examine embryonic stage-specific effects of Nkx2-5, tamoxifen-inducible Nkx2-5 knockout mice<sup>23</sup> were analysed with several lines of control mice. This study focuses on Nkx2-5 ablation beginning at E12.5 when the septum secundum starts to grow,<sup>21</sup> in which defects are observed in human NKX2-5 mutations.

To avoid the effects of maternal cardiac dysfunction during pregnancy due to the loss of Nkx2-5,<sup>28</sup> tamoxifen was injected into pregnant females (flox/flox) mated with male (flox/flox/Cre) mice. All Nkx2-5-ablated embryos were alive at E16.5. However, at E17.5, no living embryos were observed (Figure 1A), indicating that the loss of Nkx2-5 causes death within 5 days after tamoxifen injection. These effects are specific for Nkx2-5 ablation in the presence of Cre-recombinase and tamoxifen injection, and were not

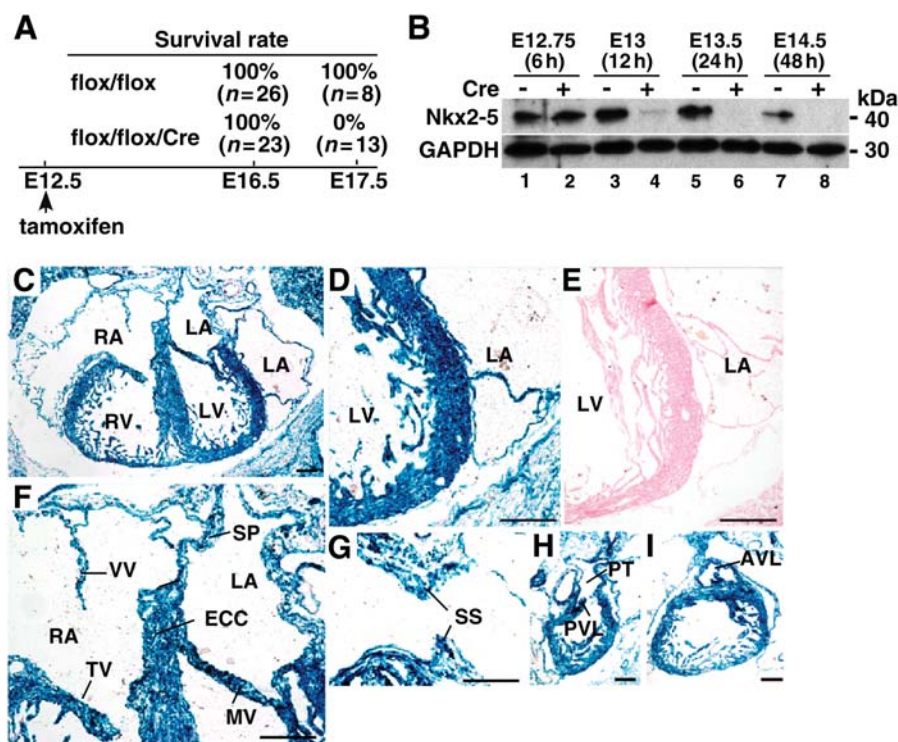


**Figure 1** Schematic of time course of tamoxifen-inducible targeting of Nkx2-5 beginning at E12.5. (A) Experimental time course of Nkx2-5 knock-out beginning at E12.5 including survival rates of flox/flox or flox/flox/Cre embryos at E16.5 and E17.5. (B) Western blotting for levels of Nkx2-5 protein in heart lysates obtained from flox/flox (lanes 1, 3, 5, 7) and flox/flox/Cre mice (lanes 2, 4, 6, 8) at E12.75 (6 h after tamoxifen injection) to E14.5 (48 h after tamoxifen injection). GAPDH expression is also shown. (C–I) E16.5 frozen heart sections of R26R/Tg-Cre-ER<sup>TM</sup> stained for  $\beta$ -galactosidase after tamoxifen injection; (C) four-chamber heart; (D) left ventricle and atrium, (E) left ventricle and atrium from R26R/Tg-Cre-ER<sup>TM</sup> negative littermate, (F) tricuspid and mitral valves, venous valve, endocardial cushion, septum primum, (G) tissue section including septum secundum, (H) right ventricle, pulmonary trunk and pulmonary valve leaflet, (I) aortic valve leaflet. Bars = 200  $\mu$ m. AVL, aortic valve leaflet; ECC, endocardial cushion; LA, left atrium; LV, left ventricle; MV, mitral valve; PT, pulmonary trunk; PVL, pulmonary valve leaflet; RA, right atrium; RV, right ventricle; SP, septum primum; SS, septum secundum; TV, tricuspid valve; VV, venous valve.

demonstrated in control embryos after tamoxifen injection (E17.5 flox/flox  $n = 8$ , or wild/wild/Cre  $n = 3$ ). Death by E17.5 after tamoxifen injection at E12.5 is specific: when tamoxifen is injected at E10.5 (2 days earlier), flox/flox/Cre embryos were found dead at E14.5 with slightly shorter crown-rump length than that of flox/flox embryos (Supplementary material online, Figure S1), whereas tamoxifen injection at E13.5 (1 day later) extends survival until shortly after birth (18 alive in a total of 22 flox/flox/Cre mice at E19.5 by Caesarean section).

Western blotting demonstrated that Nkx2-5 protein expression was not changed in flox/flox/Cre hearts at 6 h (E12.75), but was markedly reduced 12 h after tamoxifen injection (E13;  $\approx 88\%$  reduction in flox/flox/Cre vs. flox/flox), and was below the level of detection 24 h after tamoxifen injection (E13.5; Figure 1B). E16.5  $\beta$ -galactosidase expression in R26R reporter mice with heterozygous Cre-ER<sup>TM</sup> after tamoxifen injection demonstrates that Cre-recombinase activity occurs throughout the heart, including atria, ventricles, endocardial cushions, valves, and right and left outflow tracts (Figure 1C–I). In 99.5% of isolated sarcomeric actinin-positive ventricular cardiomyocytes, Nkx2-5 expression was below the level of detection (Nkx2-5 positive nuclei  $n = 13$  in total nuclei  $n = 2470$ ). These results indicate that Nkx2-5 expression in the hearts was globally and almost completely eliminated shortly

after tamoxifen injection. Of note, this knockout model is stage-specific rather than cardiomyocyte-specific deletion of Nkx2-5 using heterozygous Cre-ER<sup>TM</sup> transgene under the control of the CMV enhancer and the chicken  $\beta$ -globin promoter.<sup>22</sup>

### 3.2 Abnormal cardiac rhythm and contraction in Nkx2-5 knockout embryos

E16.5 Nkx2-5 knockout embryos were oedematous with accumulation of fluid in subcutaneous regions, which is often associated with heart failure in embryos (Figure 2A). E16.5 crown-rump length is comparable between flox/flox vs. flox/flox/Cre embryos, suggesting that Nkx2-5 deficiency does not affect the overall growth by E16.5 and that disease progression leading to death is rapid (Figure 2B).

*In utero* echocardiography demonstrates reduced cardiac contraction in Nkx2-5 knockout embryos (Figure 2C, and Table 1). In addition, irregular ventricular contraction, reduced heart rate (averaged), and dissociation of atrio-ventricular (AV) contraction were demonstrated in these embryos (Figure 2C, Table 1, and Supplementary material online, Movies). Whether irregular ventricular contractions are only due to AV block remain to be clarified by ECG recordings obtained from embryos *in utero*.

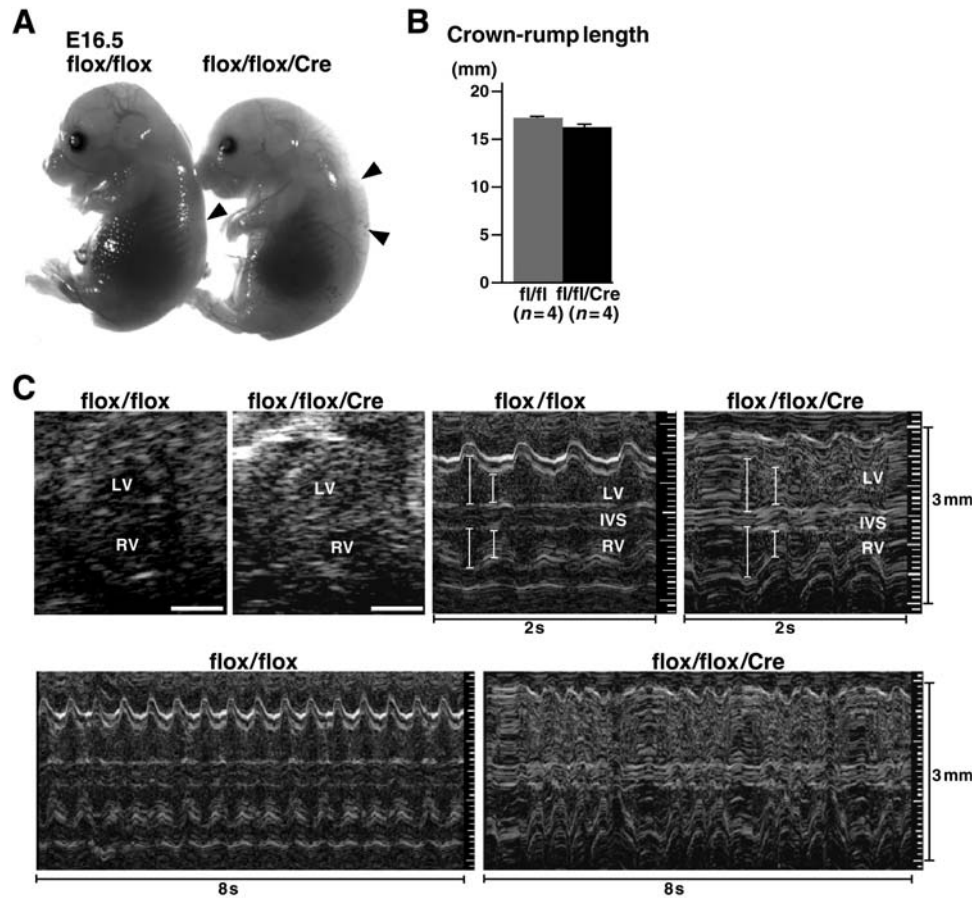


**Figure 2** Body size and echocardiographic analysis of E16.5 embryos. (A) E16.5 flox/flox (left) and flox/flox/Cre (right) littermates. Subcutaneous oedema is demonstrated in flox/flox/Cre embryos (compare arrowheads). (B) Crown-rump length is not different between flox/flox vs. flox/flox/Cre littermates ( $n = 4$  each). (C) Representative imaging of B- and M-mode (2 and 8 s) ultrasound biomicroscope. Irregular ventricular contraction is demonstrated in M-mode images. See Table 1 for cardiac indices and Supplementary material online, Video. fl, flox; IVS, inter-ventricular septum.

### 3.3 Thin ventricular wall and septum defects in Nkx2-5-ablated embryos

Histological examination was performed using serial transverse tissue sections (5  $\mu\text{m}$  thickness; E16.5, flox/flox  $n = 11$ , flox/flox/Cre  $n = 8$ ). Consistent with physiological analyses, Nkx2-5-ablated hearts were enlarged and were characterized by a thinner outer cardiac layer (compact layer) in the left ventricular free wall (Figure 3A and C vs. B and D). Large VSDs ( $>145 \mu\text{m}$ , 29 sections) were found in 38% of the flox/flox/Cre mice ( $n = 3$  in 8 embryos), while small membranous VSDs were found in 27% of flox/flox mice ( $n = 3$  in 11 embryos; Figure 3A, E, G vs. B, F, H). Small membranous VSD observed in flox/flox embryos could be due to a modification of the Nkx2-5 alleles during insertion of loxP sites in intronic and 3' non-coding sequences. In our previous study using neonatal hearts, Nkx2-5 mRNA expression was slightly higher in flox/flox mice compared with wild-type littermates.<sup>23</sup> Right and left ventricular outflow tracts were comparable between flox/flox vs. flox/flox/Cre embryos (Figure 3I, K, M, O vs. J, L, N, P).

Representative tissue sections of septum secundum demonstrate that the anterior/frontal part of septum secundum consists of a continuous thick muscular structure, followed by the appearance of a gap in the middle of the septum (foramen ovale; Figure 4A and B vs. F and

**Table 1** Echocardiographic indices of control (flox/flox) vs. Nkx2-5 knockout (flox/flox/Cre) at E16.5 (mean  $\pm$  SE)

	flox/flox ( $n = 8$ )	flox/flox/Cre ( $n = 10$ )
HR (b.p.m.)	131 $\pm$ 6	115 $\pm$ 7
LVDd (mm)	0.69 $\pm$ 0.03	0.79 $\pm$ 0.08
LVDs (mm)	0.26 $\pm$ 0.02	0.43 $\pm$ 0.03*
%FS	63 $\pm$ 2	45 $\pm$ 4*
LV area (diastolic) (mm <sup>2</sup> )	0.62 $\pm$ 0.06	0.71 $\pm$ 0.08
LV area (systolic) (mm <sup>2</sup> )	0.17 $\pm$ 0.02	0.29 $\pm$ 0.04*
%fractional area change	73 $\pm$ 2	59 $\pm$ 4*
No. of mice with irregular ventricular contraction (%)	0 (0)	6 (60)
Mother's HR (b.p.m.)	391 $\pm$ 11	395 $\pm$ 10

LVD, left ventricular diameter. \* $P < 0.05$ .

G). The posterior/dorsal part of the foramen ovale is covered by septum primum (Figure 4E and J), which is located slightly to the left of the septum secundum.<sup>21,29</sup> In control flox/flox heart, the

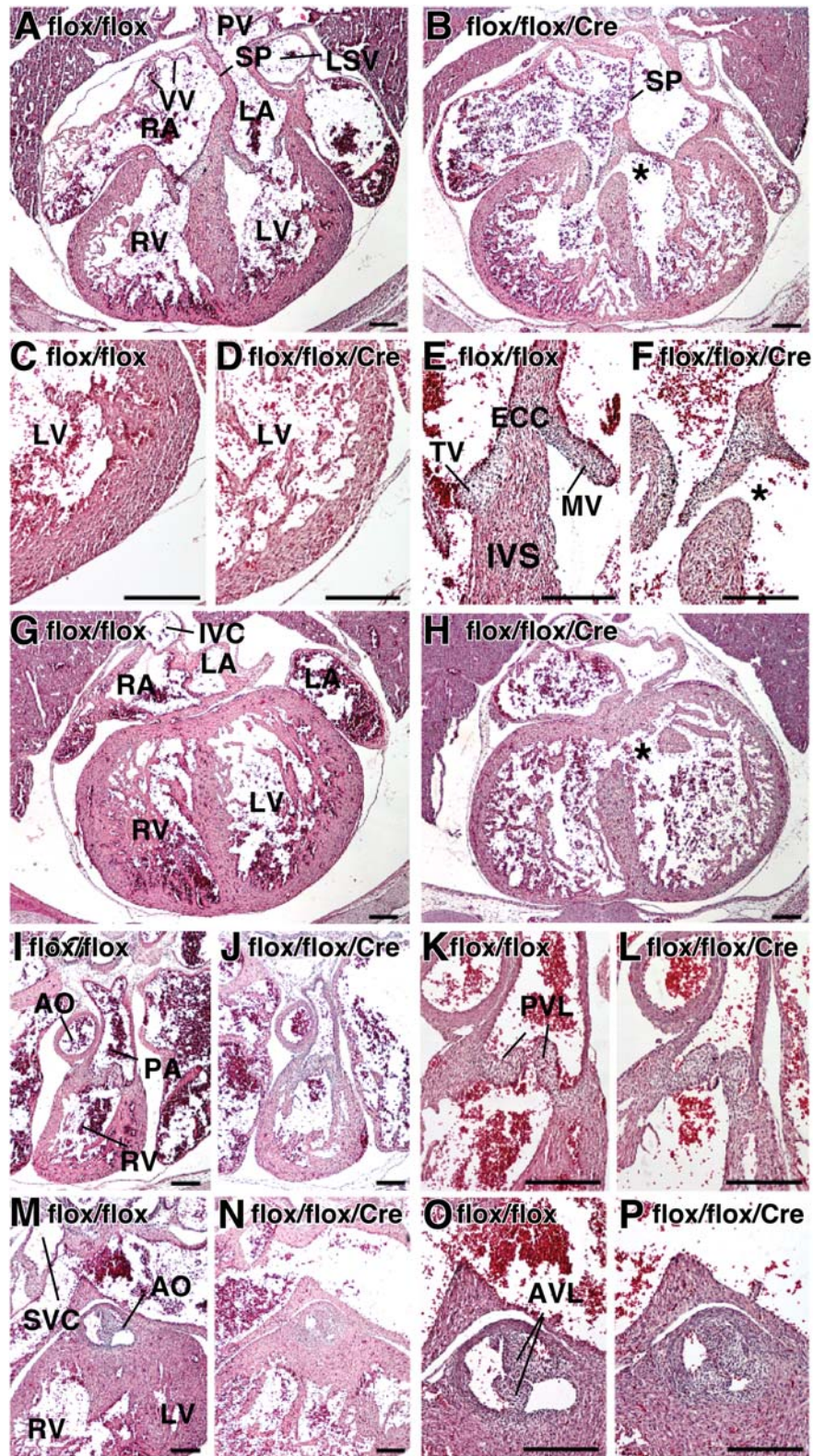


**Figure 3** Cardiac morphologies in E16.5 Nkx2-5 knockout embryos. (A–P) HE-stained serial tissue sections of E16.5 flox/flox and flox/flox/Cre embryos. (A and B) four-chamber heart, VSD in flox/flox/Cre embryo is marked with \*; (C and D) left ventricles; (E and F) endocardial cushion and inter-ventricular septum; (G and H) four-chamber heart posterior/dorsal of the sections (A and B) including inferior vena cava connection to right atrium. Additional VSD in flox/flox/Cre (marked with \*). (I and J) right ventricle to pulmonary trunk; (K and L) pulmonary valve leaflets; (M and N) left ventricular outflow; (O and P) aortic valve leaflets. Bars = 200  $\mu$ m. AO, aorta; IVC, inferior vena cava; LSV, left superior vena cava; PA, pulmonary artery; PV, pulmonary vein; SVC, superior vena cava.

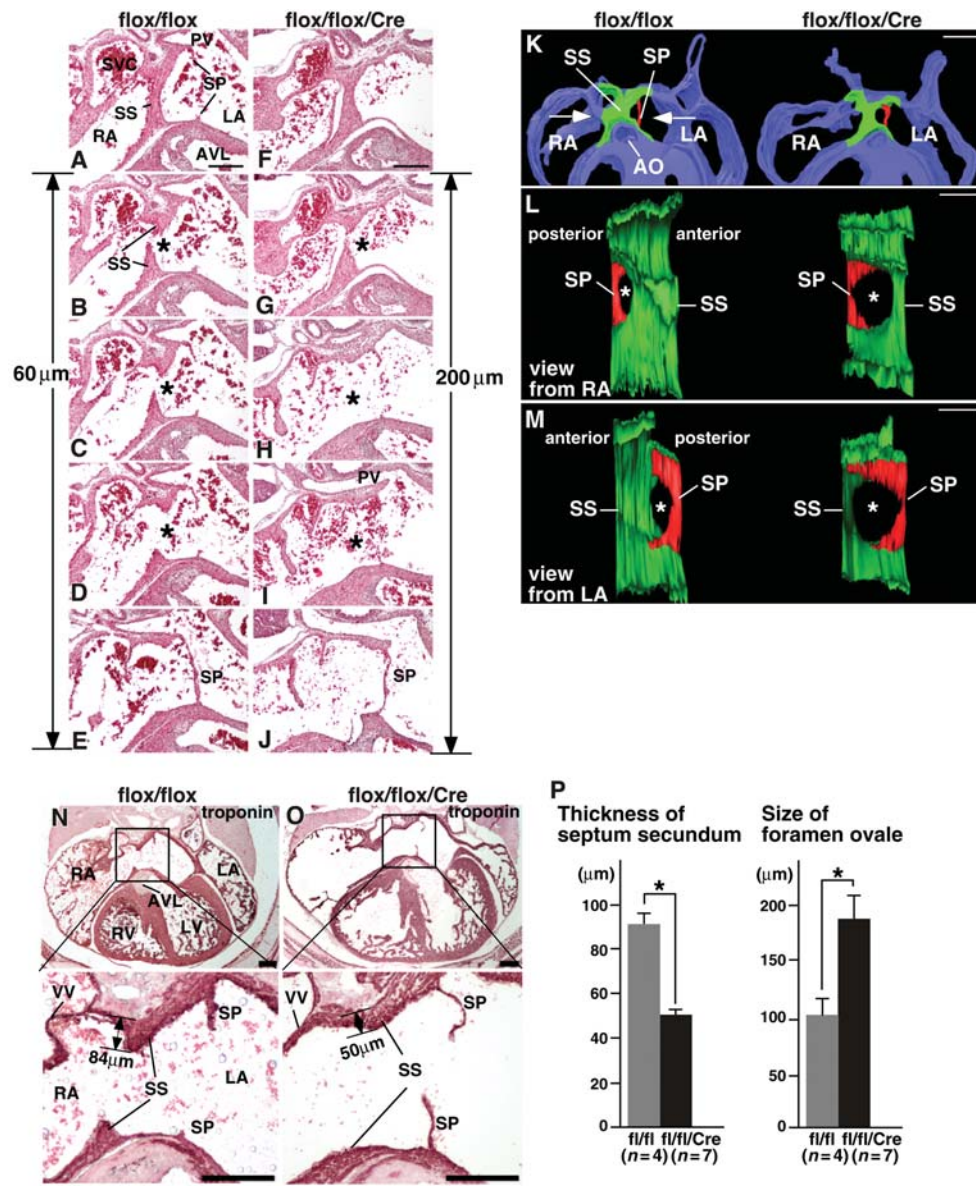


**Figure 4** Morphology of septum secundum in E16.5 *Nkx2-5* knockout embryos. (A–J) Histological sections from *flox/flox* (A–E) and *flox/flox/Cre* hearts (F–J). Anterior/frontal sections (top panel) to posterior/dorsal (bottom panels) are shown. Calculated size of foramen ovale is shown. (K–M) 3D reconstructed foramen ovale including a part of septum secundum and primum. (N and O) Troponin T-stained tissue sections at a similar plane including venous valves and part of LV outflow that demonstrate that the length of septum secundum from the atrial roof is 84 μm in *flox/flox* vs. 50 μm in *flox/flox/Cre* embryos. (P) Thickness of the troponin-positive septum secundum and size of foramen ovale calculated from a number of tissue sections which include foramen ovale. *flox/flox*, *n* = 4; *flox/flox/Cre*, *n* = 7. Bars = 500 μm in panel K; other bars = 200 μm.

distance from the opening to the closure by septum primum is 60 μm (12 serial sections). In *Nkx2-5*-ablated heart, it was increased to 200 μm, and the protrusion of the septum secundum both from the atrial roof (superior/cranial) and endocardial cushion (inferior/caudal) was smaller (see Figure 4K–P).

Reconstructed three-dimensional (3D) images of septum secundum and primum demonstrated increased size of the foramen ovale in *flox/flox/Cre* heart (Figure 4K–M). In multiple embryos, the thickness of troponin-positive muscle layer from the atrial roof to the leading edge of the septum secundum was smaller in *Nkx2-5*-ablated embryos at a similar section plane, including venous valves and part of

LV outflow tract (Figure 4N vs. O). Size of the foramen ovale (antero-posterior axis) calculated by the number of slides (5 μm thickness) was larger in *Nkx2-5*-ablated hearts (Figure 4P).

Expression of the cellular proliferation marker serine 10-phosphorylated histone H3 (Figure 5A and B) and cell-death markers [TUNEL (Figure 5C and D) or activated cleaved caspase 3, data not shown] was not statistically different in multiple control and *Nkx2-5*-ablated hearts (*n* > 2 each). Only a few TUNEL- and phospho-H3 positive cells were recognized in the atrial wall including the superior/cranial part of the septum secundum: TUNEL positive cells were 2 of 345 nuclei (0.58%) in *flox/flox*

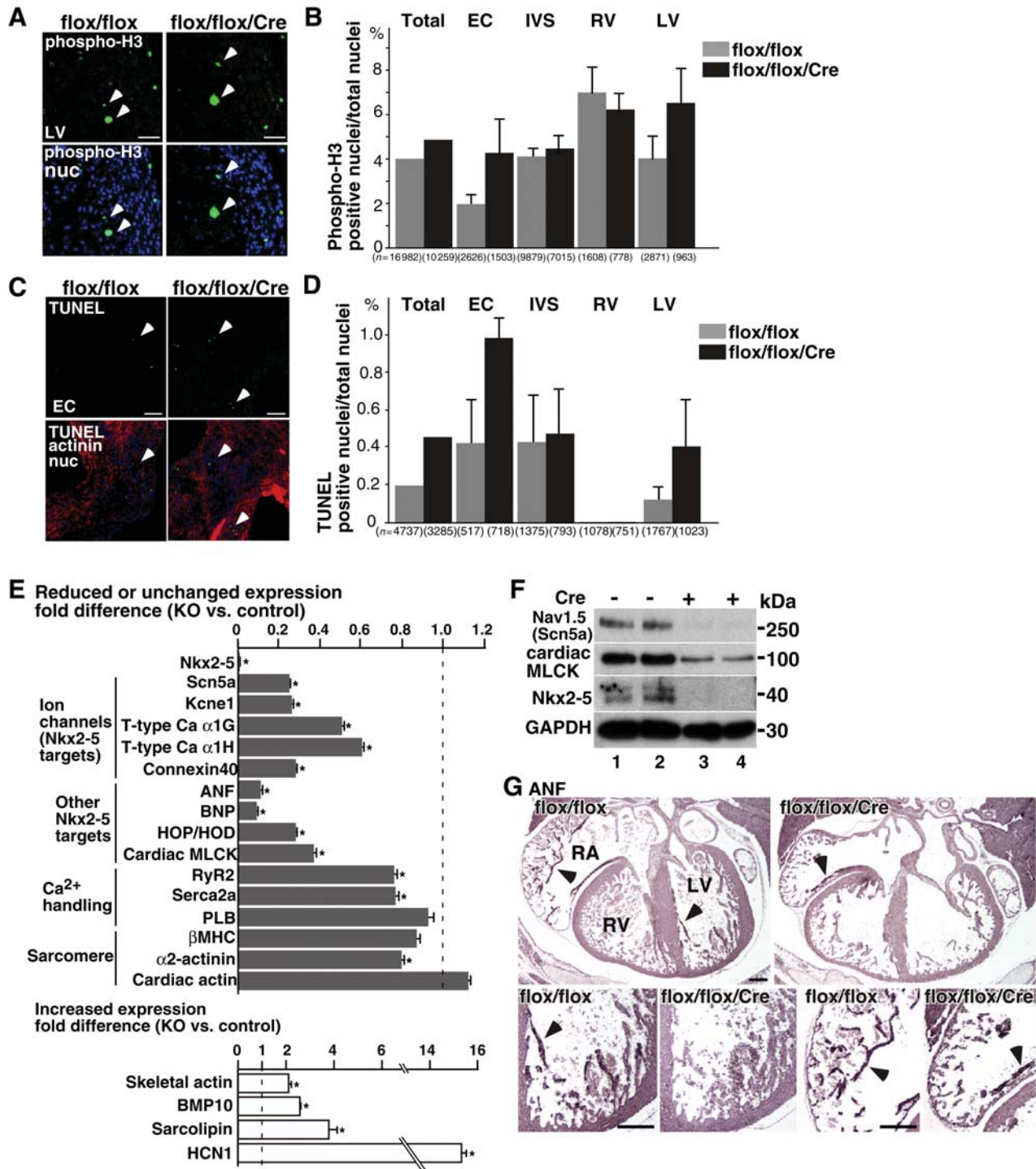


**Figure 5** Expression of proliferation and apoptosis markers, transcripts, and proteins in Nkx2-5 knockout embryos. (A) Phospho-histone 3 staining of LV wall tissue sections. Arrowheads indicate phospho H3-positive proliferating cells. (B) Summarized data (mean ± SE) of phospho-H3 positive nuclei (% to a total nuclei) obtained from multiple tissue sections. Number of the nuclei examined is indicated. (C) TUNEL staining of the tissue sections including endocardial cushion. (D) Summarized data (mean ± SE) of TUNEL positive nuclei (% of total nuclei) obtained from multiple tissue sections. (E) Real-time RT-PCR demonstrates decreased or unchanged transcripts (grey bars) or increased transcripts (white bars) in Nkx2-5 knockout embryos. (F) Western blotting demonstrates reduction of Na<sub>v</sub>1.5(α) and cardiac MLCK proteins in Nkx2-5-ablated hearts (lanes 1 vs. 2 and 3 vs. 4). (G) Immunostaining of ANF demonstrating reduced ANF protein in ventricular trabeculae (arrows) and atria (arrowheads) of Nkx2-5 knockout mice. Bars = 50 μm in panels A, C; bars = 200 μm in panel G. EC, endocardial cushion.

flox vs. 1 of 477 (0.21%) in flox/flox/Cre; phospho-H3 positive cells were 2 of 314 (0.64%) in flox/flox vs. 5 of 715 (0.70%) in flox/flox/Cre hearts.

In summary, histological analyses demonstrate cardiac enlargement, thin ventricular wall, and abnormal septum morphology in Nkx2-5-ablated hearts. Rates of cell proliferation and death were not significantly changed in the absence of Nkx2-5.

### 3.4 Abnormal expression of transcripts and proteins

To understand the underlying mechanisms contributing to contraction and conduction abnormalities in Nkx2-5-ablated embryos, the expression of a series of known Nkx2-5 downstream transcripts, as well as several transcripts critical for calcium handling and sarcomere formation was examined. More than 70% reduction in transcripts of several ion channels necessary for electrical polarization of cardiomyocytes, including Na<sub>v</sub>1.5- $\alpha$  subunit (Scn5a), Kcne1/minK, and connexin 40, as well as ~40% reduction of T-type Ca<sup>2+</sup> channels ( $\alpha$ 1H,  $\alpha$ 1G) were demonstrated in Nkx2-5-ablated hearts 4 days after tamoxifen injection (Figure 5E). Expression of other Nkx2-5 downstream targets, including atrial natriuretic factor (ANF), brain natriuretic peptide, homeodomain only protein (HOP/HOD), and cardiac myosin light chain kinase (MLCK), was also decreased by 63–90% in Nkx2-5 knockout embryos (Figure 5E). The transcriptional profile is similar to that with perinatal ablation of Nkx2-5.<sup>23</sup> In contrast, increased expression of bone morphogenetic protein 10 (BMP10; 2.6-fold), sarcolipin (3.8-fold), and hyperpolarization-activated cyclic-nucleotide-modulated channel 1 (14.9-fold) was demonstrated to be consistent with that found in the previous study.<sup>15</sup>

Na<sub>v</sub>1.5 is the primary cardiac Na<sup>+</sup> channel, which regulates the rapid depolarization of contractile myocardium. Western blotting confirmed a marked reduction in channel pore-forming  $\alpha$ -subunit, Na<sub>v</sub>1.5( $\alpha$ ), which may contribute to conduction and potential contraction defects in Nkx2-5-ablated embryos (Figure 5F). Cardiac MLCK is involved in sarcomere organization and regulation of cardiac contraction,<sup>27,30,31</sup> which is also reduced in Nkx2-5-ablated embryos (Figure 5F). ANF plays important roles in the maintenance of fluid and electrolyte balance as well as cardiovascular growth.<sup>32,33</sup> Immunostaining demonstrates ANF expression at the inner layer (trabecular layer) of ventricles (Figure 5G, arrow) and in the atria (Figure 5G, arrowhead) in flox/flox heart, but it is only sparsely detected in flox/flox/Cre hearts.

### 3.5 Reduced AchE activity in ventricular trabeculae

The formation of ventricular conduction systems in Nkx2-5-ablated hearts was examined by AchE activity, which is observed predominantly in the ventricular trabeculae and inner layer of atria at E16.5 (Figure 6A). AchE activity is known to coincide with parts of the developing ventricular conduction system and probably controls conduction of electrical impulse during embryonic stages as demonstrated in rat and chick, which is different from autonomic nervous system innervation to the nodal tissues in postnatal hearts.<sup>34–36</sup>

AchE staining in ventricular trabeculae was slightly weaker in flox/flox/Cre than flox/flox hearts under the same experimental conditions (Figure 6A, Supplementary material online, Figure S2). Also,

the proximal portion of the ventricular conduction system located at the leading edge of the ventricular septum was smaller in Nkx2-5-ablated hearts estimated by the number of AchE-positive sections (1 section 'anterior' to the AchE-positive section to the end of the positive staining 'posterior', Figure 6A). AchE-positive staining was observed at 180  $\mu$ m thickness in flox/flox hearts and was 50  $\mu$ m in flox/flox/Cre hearts (Figure 6A), which is significantly different ( $170 \pm 6$  vs.  $50 \pm 6$   $\mu$ m, respectively,  $n = 3$  each group,  $P < 0.05$ ). Therefore, AchE-positive ventricular conduction system is morphologically changed after ablation of Nkx2-5, which may contribute to conduction defects.

### 3.6 Ca<sup>2+</sup> handling and cell motion in Nkx2-5-ablated embryonic cardiomyocytes

Cardiac conduction and contraction are closely coupled. Reduction of Na<sub>v</sub>1.5( $\alpha$ ) alone causes contraction defects as in human patients with SCN5A mutations.<sup>37,38</sup> In addition, an ~22% reduction of ryanodine receptor 2 (RyR2) and sarco-endoplasmic reticulum Ca<sup>2+</sup> ATPase 2a (SERCA2a) mRNA in Nkx2-5-ablated hearts was demonstrated (Figure 5E), which may affect Ca<sup>2+</sup> release and uptake for cardiac contraction/relaxation. Expression of mRNA for the inhibitor of SERCA2a, phospholamban, was not significantly changed; however, that of sarcolipine was increased 3.8-fold, which is not normally expressed in ventricles.<sup>39,40</sup>

Indeed, ventricular cardiomyocytes isolated from E15.5 flox/flox/Cre embryos demonstrate reduced speed of contraction and relaxation accompanied by increased time for Ca<sup>2+</sup> release and decay without affecting Ca<sup>2+</sup> amplitude (Figure 6B and C). These results are similar to those obtained with sarcolipin-overexpressing cardiomyocytes.<sup>41,42</sup>

Sarcomere structure is less organized in Nkx2-5-ablated cardiomyocytes as revealed by thin sarcomeric bundles detected by phalloidin (Figure 6D). Phalloidin intensity was reduced by 51% in Nkx2-5 knockout cardiomyocytes (Figure 6E), suggesting that the loss of Nkx2-5 affects the formation or maintenance of sarcomere structure. A similar abnormal sarcomere structure was observed in cardiac MLCK knocked-down cardiomyocytes.<sup>27</sup> The expression of additional transcripts of sarcomeres is shown in Figure 5E.

## 4. Discussion

With respect to the pathogenesis of human congenital heart disease associated with NKX2-5 mutations, all the phenotypes demonstrated in human patients are also found in mice in which Nkx2-5 is ablated at mid-embryonic stage (E12.5), including cardiac anomalies, conduction, and contraction defects. Nkx2-5-ablated embryos die within 5 days after tamoxifen injection (E17.5) with heart failure.

The pathogenesis underlying embryonic lethality with contraction and conduction defects in Nkx2-5 knockout embryos is likely attributed to altered expression of multiple Nkx2-5 downstream targets acting in combination. In fact, embryonic lethality was demonstrated with homozygous gene deletion of Scn5a encoding the cardiac sodium channel Na<sub>v</sub>1.5 by E10.5,<sup>43</sup> and HOP/HOD between E10.5 and E12.5 with incomplete penetrance.<sup>44,45</sup> Na<sub>v</sub>1.5 is the primary cardiac Na<sup>+</sup> channel isoform, which regulates rapid depolarization of contractile myocardium. Recently, an additional non-electrogenic role for Na<sup>+</sup> channels in heart development was demonstrated in zebrafish.<sup>46</sup>



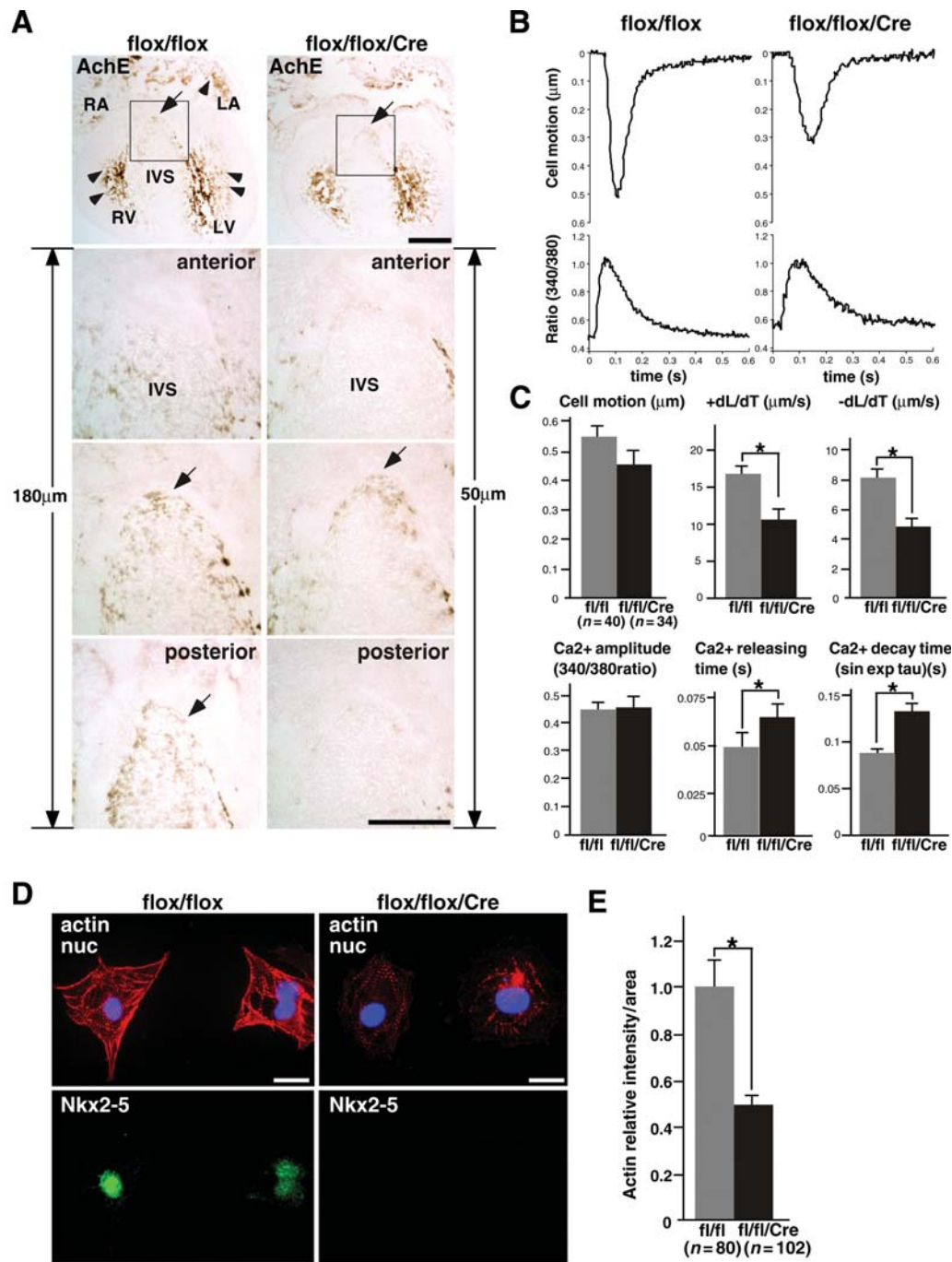


**Figure 6** Reduced AchE activities, contraction, and Ca<sup>2+</sup> handling defects in Nkx2-5 knockout hearts. (A) Distribution of AchE activity in E16.5 embryos predominantly in the ventricular trabeculae and inner layer of atria both in flox/flox and flox/flox/Cre heart (top panel, brown staining, arrowheads). AchE-positive area at the leading edge of ventricular septum (arrows) is smaller in Nkx2-5-ablated hearts. Counting the number of sections from one section anterior to the AchE-positive section (anterior) to the end of positive staining (posterior) which was 18 sections (180  $\mu$ m) in flox/flox hearts and five sections (50  $\mu$ m) in flox/flox/Cre hearts. Bars = 500  $\mu$ m in top panels and 200  $\mu$ m in bottom panels. (B) Representative tracings of a single contraction (top) and simultaneous Ca<sup>2+</sup> transients (bottom) in an isolated cardiomyocyte from control flox/flox (left panels) or Nkx2-5 knockout (flox/flox/Cre) embryos (right panels). (C) Summarized data (mean  $\pm$  SE) obtained from multiple cardiomyocytes in two independent experiments. Nkx2-5 knockout cardiomyocytes have decreased cell motion ( $P = 0.12$ ), significantly decreased +dL/dT (speed of contraction) and -dL/dT (speed of relaxation). Increased time to 50% peak Ca<sup>2+</sup> release and Ca<sup>2+</sup> decay time without affecting total Ca<sup>2+</sup> amplitude was observed in Nkx2-5 knockout cardiomyocytes. \* $P < 0.01$ . (D) Co-immunostaining of phalloidin (actin), Nkx2-5, and DAPI showing reduced phalloidin intensity in ventricular cardiomyocytes from Nkx2-5 knockout embryos. (E) Relative intensity of phalloidin staining in individual cardiomyocyte is shown with the value in control cardiomyocytes defined as 1 (mean  $\pm$  SE). Bars = 20  $\mu$ m.

Cardiac conduction abnormalities were demonstrated in hetero- or homozygous mice with ablation of connexin40, T-type Ca channels  $\alpha 1G$ , and cardiac sodium channel  $Na_v1.5$ .<sup>43,47–49</sup>  $Ca^{2+}$  handling defects accompanied by reduced contraction were demonstrated in sarcolipin-overexpressing mice.<sup>42</sup> The profile of transcripts is similar to that in previous studies, including mice with perinatal loss of Nkx2-5.<sup>14,15,23,50,51</sup> However, a faster and greater magnitude of reduction was demonstrated in embryos with Nkx2-5 ablation beginning at E12.5 than in the perinatal period, which partly explains rapid disease progression in Nkx2-5-ablated embryos beginning at E12.5.

AchE-positive ventricular trabeculae, which likely represent components of the developing ventricular conduction system, are also morphologically changed after ablation of Nkx2-5. Therefore, reduction of transcripts expressed in the ventricular conduction system (e.g. connexin40) might be due to transcriptional down-regulation as well as under-developed ventricular conduction systems in Nkx2-5-ablated hearts, as demonstrated previously.<sup>18,52,53</sup> Reduction of AchE expression could increase the levels of acetylcholine in the cardiomyocytes, which might also functionally affect the electrical propagation<sup>34,54,55</sup> in Nkx2-5-ablated hearts.

A reduction in growth of the septum secundum and an enlarged foramen ovale in both anterior-posterior and cranial-caudal axes were observed in Nkx2-5-ablated embryos. Rates of cell death or proliferation were not significantly changed in Nkx2-5-ablated hearts, suggesting that abnormal structural arrangements, such as folding of atrial myocardium, may play a role in this cardiac anomaly. Septum anomalies were demonstrated in connexin40 hetero- and homozygous knockout mice,<sup>56</sup> and the expression of connexin40 was reduced by 70% in Nkx2-5 knockout embryos. The mechanisms by which the loss of gap junction protein connexin40 resulted in a reduced propagation of action potential and ASD remain to be elucidated. Additional factors, including abnormal blood flow in the heart itself by contraction defects,<sup>3</sup> may also be involved in cardiac anomaly in Nkx2-5-ablated embryos.

Septum secundum anomalies are observed in all embryos after ablation of Nkx2-5 beginning at E12.5 in this study, which is substantially higher than those seen with heterozygous germline deletion of Nkx2-5 gene (around 1 and 18%).<sup>16–19</sup> One interpretation of these observations is that Nkx2-5 expression has dose-dependent effects on septum formation in mice. Higher penetrance of ASD in human patients with heterozygous NKX2-5 mutations (~80%)<sup>4–7</sup> could be specific for humans. Another explanation is that NKX2-5 mutations are not silent, and may be involved in NKX2-5-dependent transcriptional regulation in either a dominant inhibitory or a hypomorphic gain-of-function manner.<sup>50</sup> For instance, introduction of Nkx2-5 mutants in *Xenopus* embryos results in small hearts, no heart formation, or cardiac anomalies.<sup>57,58</sup> Analysis of the knock-in mouse that harbours heterozygous point mutant allele of Nkx2-5 would be helpful for clarification.

Cardiac anomalies were absent in MLC2v-Cre induced Nkx2-5 gene ablations, in which Nkx2-5 expression is eliminated in the ventricular cardiomyocytes starting around E8.0.<sup>15</sup> This suggests that deletion of Nkx2-5 in cell types other than committed-ventricular cardiomyocytes, such as cushion mesenchymal or epicardial-derived mesenchymal cells, may play a critical role in cardiac anomalies at least for ventricular septum abnormalities or thin ventricular wall.<sup>59–62</sup> Neural-crest-derived mesenchymal cells contributing to septation of the outflow tracts are distributed to these regions in the earlier stage (E9.5–12.5).<sup>63</sup> Nkx2-5 ablation

after E12.5 did not demonstrate apparent anomalies in the right and left outflow tracts.

Ventricular hypertrabeculation was demonstrated in MLC2v-Cre-induced Nkx2-5 gene ablation due to overexpression of BMP10, which is normally expressed transiently in the ventricular trabecular myocardium from E9.0 to E13.5.<sup>15,64</sup> However, this was not found in E16.5 flox/flox/Cre embryos with tamoxifen injection at E12.5 in this study or in E9.5 germline deletion of Nkx2-5 embryos.<sup>14</sup> The discrepancy among these studies could be due to timing of Nkx2-5-ablation. When tamoxifen was injected at E10.5, Nkx2-5-ablation resulted in embryonic lethality by E14.5 with hypertrabeculation (Supplementary material online, Figure S1).

In summary, we demonstrated that Nkx2-5 is necessary for murine survival after E12.5 by regulating the expression of critical genes for cardiac contraction, conduction, and morphogenesis. Global deletion of Nkx2-5 beginning from the mid-embryonic stage demonstrated a substantially different spectrum of cardiac abnormalities leading to embryonic death, which was not demonstrated in ventricular myocyte-specific Nkx2-5 gene targeting.

## Supplementary material

Supplementary material is available at *Cardiovascular Research* online.

## Acknowledgements

We greatly appreciate E. Weinberg, K. Fortin, P. Sayeski, and E. Chan for valuable suggestions and technical support.

**Conflict of interest:** none declared.

## Funding

This work was funded by the National Institutes of Health (HL081577 to H.K.).

## References

- Hoffman JJ, Kaplan S, Liberthson RR. Prevalence of congenital heart disease. *Am Heart J* 2004;**147**:425–439.
- Capozzi G, Caputo S, Pizzuti R, Martina L, Santoro M, Santoro G et al. Congenital heart disease in live-born children: incidence, distribution, and yearly changes in the Campania Region. *J Cardiovasc Med (Hagerstown)* 2008;**9**:368–374.
- Andelfinger G. Genetic factors in congenital heart malformation. *Clin Genet* 2008;**73**:516–527.
- Schott JJ, Benson DW, Basson CT, Pease W, Silberbach GM, Moak JP et al. Congenital heart disease caused by mutations in the transcription factor NKX2-5. *Science* 1998;**281**:108–111.
- Benson DW, Silberbach GM, Kavanaugh-McHugh A, Cottrill C, Zhang Y, Riggs S et al. Mutations in the cardiac transcription factor NKX2.5 affect diverse cardiac developmental pathways. *J Clin Invest* 1999;**104**:1567–1573.
- Kasahara H, Benson DW. Biochemical analyses of eight NKX2.5 homeodomain missense mutations causing atrioventricular block and cardiac anomalies. *Cardiovasc Res* 2004;**64**:40–51.
- Konig K, Will JC, Berger F, Muller D, Benson DW. Familial congenital heart disease, progressive atrioventricular block and the cardiac homeobox transcription factor gene NKX2.5: identification of a novel mutation. *Clin Res Cardiol* 2006;**95**:499–503.
- Harvey RP. NK-2 homeobox genes and heart development. *Dev Biol* 1996;**178**:203–216.
- Harvey RP, Rosenthal N. *Heart Development*. San Diego, CA, USA: Academic Press; 1999.
- Lints TJ, Parsons LM, Hartley L, Lyons I, Harvey RP. Nkx-2.5: a novel murine homeobox gene expressed in early heart progenitor cells and their myogenic descendants. *Development* 1993;**119**:419–431.
- Komuro I, Izumo S. Csx: a murine homeobox-containing gene specifically expressed in the developing heart. *Proc Natl Acad Sci USA* 1993;**90**:8145–8149.
- Kasahara H, Bartunkova S, Schinke M, Tanaka M, Izumo S. Cardiac and extracardiac expression of Csx/Nkx2.5 homeodomain protein. *Circ Res* 1998;**82**:936–946.

13. Lyons I, Parsons LM, Hartley L, Li R, Andrews JE, Robb L et al. Myogenic and morphogenetic defects in the heart tubes of murine embryos lacking the homeo box gene Nkx2-5. *Genes Dev* 1995;**9**:1654–1666.
14. Tanaka M, Chen Z, Bartunkova S, Yamasaki N, Izumo S. The cardiac homeobox gene Csx/Nkx2.5 lies genetically upstream of multiple genes essential for heart development. *Development* 1999;**126**:1269–1280.
15. Pashmforoush M, Lu JT, Chen H, Amand TS, Kondo R, Pradervand S et al. Nkx2-5 pathways and congenital heart disease; loss of ventricular myocyte lineage specification leads to progressive cardiomyopathy and complete heart block. *Cell* 2004;**117**:373–386.
16. Biben C, Weber R, Kesteven S, Stanley E, McDonald L, Elliott DA et al. Cardiac septal and valvular dysmorphogenesis in mice heterozygous for mutations in the homeobox gene Nkx2-5. *Circ Res* 2000;**87**:888–895.
17. Tanaka M, Berul CI, Ishii M, Jay PY, Wakimoto H, Douglas P et al. A mouse model of congenital heart disease: cardiac arrhythmias and atrial septal defect caused by haploinsufficiency of the cardiac transcription factor Csx/Nkx2.5. *Cold Spring Harb Symp Quant Biol* 2002;**67**:317–325.
18. Jay PY, Harris BS, Maguire CT, Buerger A, Wakimoto H, Tanaka M et al. Nkx2-5 mutation causes anatomic hypoplasia of the cardiac conduction system. *J Clin Invest* 2004;**113**:1130–1137.
19. Winston JB, Erlich JM, Green CA, Aluko A, Kaiser KA, Takematsu M et al. Heterogeneity of genetic modifiers ensures normal cardiac development. *Circulation* 2010;**121**:1313–1321.
20. Wessels A, Anderson RH, Markwald RR, Webb S, Brown NA, Viragh S et al. Atrial development in the human heart: an immunohistochemical study with emphasis on the role of mesenchymal tissues. *Anat Rec* 2000;**259**:288–300.
21. Savolainen SM, Foley JF, Elmore SA. Histology atlas of the developing mouse heart with emphasis on E11.5 to E18.5. *Toxicol Pathol* 2009;**37**:395–414.
22. Hayashi S, McMahon AP. Efficient recombination in diverse tissues by a tamoxifen-inducible form of Cre: a tool for temporally regulated gene activation/inactivation in the mouse. *Dev Biol* 2002;**244**:305–318.
23. Briggs LE, Takeda M, Cuadra AE, Wakimoto H, Marks MH, Walker AJ et al. Perinatal loss of Nkx2-5 results in rapid conduction and contraction defects. *Circ Res* 2008;**103**:580–590.
24. Hogan B, Beddingtm R, Costantini F, Lacy E. *Manipulating the Mouse Embryo*. New York, NY: Cold Spring Harbor Laboratory Press; 1994.
25. El-Badawi A, Schenk EA. Histochemical methods for separate, consecutive and simultaneous demonstration of acetylcholinesterase and norepinephrine in cryostat sections. *J Histochem Cytochem* 1967;**15**:580–588.
26. Soufan AT, Ruijter JM, van den Hoff MJ, de Boer PA, Hagoort J, Moorman AF. Three-dimensional reconstruction of gene expression patterns during cardiac development. *Physiol Genomics* 2003;**13**:187–195.
27. Chan JY, Takeda M, Briggs LE, Graham ML, Lu JT, Horikoshi N et al. Identification of cardiac-specific myosin light chain kinase. *Circ Res* 2008;**102**:571–580.
28. Takeda M, Briggs LE, Wakimoto H, Marks MH, Warren SA, Lu JT et al. Slow progressive conduction and contraction defects in loss of Nkx2-5 mice after cardiomyocyte terminal differentiation. *Lab Invest* 2009;**89**:983–993.
29. Petiet AE, Kaufman MH, Goddeeris MM, Brandenburg J, Elmore SA, Johnson GA. High-resolution magnetic resonance histology of the embryonic and neonatal mouse: a 4D atlas and morphologic database. *Proc Natl Acad Sci USA* 2008;**105**:12331–12336.
30. Seguchi O, Takashima S, Yamazaki S, Asakura M, Asano Y, Shintani Y et al. A cardiac myosin light chain kinase regulates sarcomere assembly in the vertebrate heart. *J Clin Invest* 2007;**117**:2812–2824.
31. Ding P, Huang J, Battiprolu PK, Hill JA, Kamm KE, Stull JT. Cardiac myosin light chain kinase is necessary for myosin regulatory light chain phosphorylation and cardiac performance in vivo. *J Biol Chem* 2010;**285**:40819–40829.
32. Houweling AC, van Borren MM, Moorman AF, Christoffels VM. Expression and regulation of the atrial natriuretic factor encoding gene Nppa during development and disease. *Cardiovasc Res* 2005;**67**:583–593.
33. McGrath MF, de Bold ML, de Bold AJ. The endocrine function of the heart. *Trends Endocrinol Metab* 2005;**16**:469–477.
34. Lamers WH, te Kortschot A, Los JA, Moorman AF. Acetylcholinesterase in prenatal rat heart: a marker for the early development of the cardiac conductive tissue? *Anat Rec* 1987;**217**:361–370.
35. Nakamura T, Ikeda T, Shimokawa I, Inoue Y, Suematsu T, Sakai H et al. Distribution of acetylcholinesterase activity in the rat embryonic heart with reference to HNK-1 immunoreactivity in the conduction tissue. *Anat Embryol (Berl)* 1994;**190**:367–373.
36. Franco D, Moorman AF, Lamers WH. Expression of the cholinergic signal-transduction pathway components during embryonic rat heart development. *Anat Rec* 1997;**248**:110–120.
37. McNair WP, Ku L, Taylor MR, Fain PR, Dao D, Wolfel E et al. SCN5A mutation associated with dilated cardiomyopathy, conduction disorder, and arrhythmia. *Circulation* 2004;**110**:2163–2167.
38. Olson TM, Michels VV, Ballew JD, Reyna SP, Karst ML, Herron KJ et al. Sodium channel mutations and susceptibility to heart failure and atrial fibrillation. *JAMA* 2005;**293**:447–454.
39. Minamisawa S, Wang Y, Chen J, Ishikawa Y, Chien KR, Matsuoka R. Atrial chamber-specific expression of sarcolipin is regulated during development and hypertrophic remodeling. *J Biol Chem* 2003;**278**:9570–9575.
40. Vangheluwe P, Schuermans M, Zador E, Waelkens E, Raeymaekers L, Wuytack F. Sarcolipin and phospholamban mRNA and protein expression in cardiac and skeletal muscle of different species. *Biochem J* 2005;**389**:151–159.
41. Babu GJ, Zheng Z, Natarajan P, Wheeler D, Janssen PM, Periasamy M. Overexpression of sarcolipin decreases myocyte contractility and calcium transient. *Cardiovasc Res* 2005;**65**:177–186.
42. Gramolini AO, Trivieri MG, Oudit GY, Kislinger T, Li W, Patel MM et al. Cardiac-specific overexpression of sarcolipin in phospholamban null mice impairs myocyte function that is restored by phosphorylation. *Proc Natl Acad Sci USA* 2006;**103**:2446–2451.
43. Papadatos GA, Wallerstein PM, Head CE, Ratcliff R, Brady PA, Benndorf K et al. Slowed conduction and ventricular tachycardia after targeted disruption of the cardiac sodium channel gene Scn5a. *Proc Natl Acad Sci USA* 2002;**99**:6210–6215.
44. Shin CH, Liu ZP, Passier R, Zhang CL, Wang DZ, Harris TM et al. Modulation of cardiac growth and development by HOP, an unusual homeodomain protein. *Cell* 2002;**110**:725–735.
45. Chen F, Kook H, Milewski R, Gitler AD, Lu MM, Li J et al. Hop is an unusual homeobox gene that modulates cardiac development. *Cell* 2002;**110**:713–723.
46. Chopra SS, Stroud DM, Watanabe H, Bennett JS, Burns CG, Wells KS et al. Voltage-gated sodium channels are required for heart development in zebrafish. *Circ Res* 2010;**106**:1342–1350.
47. Kirchhoff S, Nelles E, Hagendorff A, Kruger O, Traub O, Willecke K. Reduced cardiac conduction velocity and predisposition to arrhythmias in connexin40-deficient mice. *Curr Biol* 1998;**8**:299–302.
48. Simon AM, Goodenough DA, Paul DL. Mice lacking connexin40 have cardiac conduction abnormalities characteristic of atrioventricular block and bundle branch block. *Curr Biol* 1998;**8**:295–298.
49. Mangoni ME, Traboulsie A, Leoni AL, Couette B, Marger L, Le Quang K et al. Bradyarrhythmia and slowing of the atrioventricular conduction in mice lacking Cav3.1/alpha1G T-type calcium channels. *Circ Res* 2006;**98**:1422–1430.
50. Kasahara H, Wakimoto H, Liu M, Maguire CT, Converso KL, Shioi T et al. Progressive atrioventricular conduction defects and heart failure in mice expressing a mutant Csx/Nkx2.5 homeoprotein. *J Clin Invest* 2001;**108**:189–201.
51. Bruneau BG, Nemer G, Schmitt JP, Charron F, Robitaille L, Caron S et al. A murine model of Holt-Oram syndrome defines roles of the T-box transcription factor Tbx5 in cardiogenesis and disease. *Cell* 2001;**106**:709–721.
52. Meysen S, Marger L, Hewett KW, Jarry-Guichard T, Agarkova I, Chauvin JP et al. Nkx2.5 cell-autonomous gene function is required for the postnatal formation of the peripheral ventricular conduction system. *Dev Biol* 2007;**303**:740–753.
53. Moskowitz IP, Kim JB, Moore ML, Wolf CM, Peterson MA, Shendure J et al. A molecular pathway including Id2, Tbx5, and Nkx2-5 required for cardiac conduction system development. *Cell* 2007;**129**:1365–1376.
54. Hall EK. Acetylcholine and epinephrine effects on the embryonic rat heart. *J Cell Physiol* 1957;**49**:187–200.
55. Robkin MA, Shepard TH, Dyer DC, Guntheroth WG. Autonomic receptors of the early rat embryo heart growth and development. *Proc Soc Exp Biol Med* 1976;**151**:799–803.
56. Gu H, Smith FC, Taffet SM, Delmar M. High incidence of cardiac malformations in connexin40-deficient mice. *Circ Res* 2003;**93**:201–206.
57. Grow MW, Krieg PA. Tinman function is essential for vertebrate heart development: elimination of cardiac differentiation by dominant inhibitory mutants of the tinman-related genes, XNkx2-3 and XNkx2-5. *Dev Biol* 1998;**204**:187–196.
58. Bartlett HL, Sutherland L, Kolker SJ, Welp C, Tajchman U, Desmarais V et al. Transient early embryonic expression of Nkx2-5 mutations linked to congenital heart defects in human causes heart defects in *Xenopus laevis*. *Dev Dyn* 2007;**236**:2475–2484.
59. Cai CL, Martin JC, Sun Y, Cui L, Wang L, Ouyang K et al. A myocardial lineage derives from Tbx18 epicardial cells. *Nature* 2008;**454**:104–108.
60. Zhou B, Ma Q, Rajagopal S, Wu SM, Doman I, Rivera-Feliciano J et al. Epicardial progenitors contribute to the cardiomyocyte lineage in the developing heart. *Nature* 2008;**454**:109–113.
61. Eisenberg LM, Markwald RR. Cellular recruitment and the development of the myocardium. *Dev Biol* 2004;**274**:225–232.
62. Snarr BS, Kern CB, Wessels A. Origin and fate of cardiac mesenchyme. *Dev Dyn* 2008;**237**:2804–2819.
63. Jiang X, Rowitch DH, Soriano P, McMahon AP, Sucov HM. Fate of the mammalian cardiac neural crest. *Development* 2000;**127**:1607–1616.
64. Chen H, Shi S, Acosta L, Li W, Lu J, Bao S et al. BMP10 is essential for maintaining cardiac growth during murine cardiogenesis. *Development* 2004;**131**:2219–2231.